Molecules and Cells

# RUNX1 Ameliorates Rheumatoid Arthritis Progression through Epigenetic Inhibition of LRRC15

Hao Ding[1,3], Xiaoliang Mei[2,3], Lintao Li[1], Peng Fang[1], Ting Guo[1], and Jianning Zhao[1,*]

[1]Department of Orthopedics, Jinling Hospital, Jinling Clinical Medical College of Nanjing Medical University, Nanjing 211166, China, [2]Department of Orthopedics, The Affiliated Taizhou People's Hospital of Nanjing Medical University, Taizhou 225300, China, [3]These authors contributed equally to this work.
*Correspondence: 2017250322@stu.njmu.edu.cn
https://doi.org/10.14348/molcells.2023.2136
www.molcells.org

**Leucine-rich repeat containing 15 (LRRC15) has been identified as a contributing factor for cartilage damage in osteoarthritis; however, its involvement in rheumatoid arthritis (RA) and the underlying mechanisms have not been well characterized. The purpose of this study was to explore the function of LRRC15 in RA-associated fibroblast-like synoviocytes (RA-FLS) and in mice with collagen-induced arthritis (CIA) and to dissect the epigenetic mechanisms involved. LRRC15 was overexpressed in the synovial tissues of patients with RA, and LRRC15 overexpression was associated with increased proliferative, migratory, invasive, and angiogenic capacities of RA-FLS and accelerated release of pro-inflammatory cytokines. LRRC15 knockdown significantly inhibited synovial proliferation and reduced bone invasion and destruction in CIA mice. Runt-related transcription factor 1 (RUNX1) transcriptionally represses *LRRC15* by binding to core-binding factor subunit beta (CBF-β). Overexpression of RUNX1 significantly inhibited the invasive phenotype of RA-FLS and suppressed the expression of proinflammatory cytokines. Conversely, the effects of RUNX1 were significantly reversed after overexpression of LRRC15 or inhibition of RUNX1-CBF-β interactions. Therefore, we demonstrated that RUNX1-mediated transcriptional repression of *LRRC15* inhibited the development of RA, which may have therapeutic effects for RA patients.**

**Keywords:** epigenetic, fibroblast-like synoviocytes, LRRC15, rheumatoid arthritis, RUNX1

## INTRODUCTION

Rheumatoid arthritis (RA) is a chronic, inflammatory autoimmune disease that predominantly affects joints (Smolen et al., 2018). RA mainly affects synovial joints, with inflammation of the synovial membrane (synovitis) characterized by angiogenesis, hyperplasia of the lining layer, and immune cell infiltration that stimulates local inflammation and, if untreated, can result in joint destruction and disability (Rivellese and Pitzalis, 2021). Progress in therapeutic approaches and understanding of RA pathogenesis have improved patient prognosis and likely remission, while partial/non-response to conventional and biologic therapies in certain patients underlines the need for new therapeutics (Sandhu and Thelma, 2022). Fibroblast-like synoviocytes (FLS) in the synovial lining develop aggressive phenotypes and are a main focus within the RA field, and the proportion of the surface marker CD90 correlates positively with the proportion of synovitis and synovial hypertrophy (Wu et al., 2021).

In the present study, we identified leucine-rich repeat containing 15 (*LRRC15*, also termed LIB) as the most significantly

Received August 31, 2022; revised November 23, 2022; accepted November 26, 2022; published online January 10, 2023

eISSN: 0219-1032

upregulated gene in the synovial tissues of RA patients (n = 16) relative to that in healthy controls (n = 7) in the Gene Expression Omnibus (GEO) database GSE77298 (https://www.ncbi.nlm.nih.gov/geo/query/acc.cgi?acc=GSE77298). Similarly, *LRRC15* was found to be one of two genes of interest identified in RA osteoblasts (Chen et al., 2017). However, its regulatory role in aggressive phenotypes of RA-FLS and RA progression remains unclear. Epigenetic characterizations, including histone modifications, open chromatin, RNA expression, and whole-genome DNA methylation, have been identified in RA-FLS (Ai et al., 2018). Intriguingly, *LRRC15* has been found to be differentially methylated and expressed in osteoarthritic cartilage and may contribute to functional and phenotypic alterations in chondrocytes (Singh et al., 2021), which link the dysregulation of LRRC15 to epigenetic modifications in skeletal disorders. Here, we focused on the transcriptional regulation of *LRRC15* in RA. Our integrated bioinformatics tools revealed that Runt-related transcription factor 1 (RUNX1) may be the transcription factor responsible for the overexpression of LRRC15 in RA. RUNX1, which functions as an important transcription factor in the pathogenesis of RA, is predicted to participate in the regulation of hub genes in RA (Xiao et al., 2022). *RUNX1* mRNA, which encodes the transcriptional partner of core-binding factor subunit beta (CBF-β), is bound and translationally regulated by CBF-β (Malik et al., 2019). In the present study, a collagen-induced arthritis (CIA) mouse model, which has clinical features similar to those of RA patients (Alabarse et al., 2018), was established, and FLS were extracted from human synovial tissues to evaluate the effect of LRRC15 on the pathological progression of RA and to elucidate the relationship between the RUNX1-CBF-β complex and LRRC15.

## MATERIALS AND METHODS

### Patients and healthy controls

This study was approved by the Institutional Review Board (IRB) of Jinling Hospital, Jinling Clinical Medical College of Nanjing Medical University (IRB No. 2022DZGZR-026). Written informed consent was obtained from all participants in compliance with the Declaration of Helsinki principles (2013). Synovial tissues were collected from 20 patients with RA who underwent knee synovectomy or total knee arthroplasty between May 2019 and March 2020. RA patients fulfilled the American College of Rheumatology criteria for RA (Aletaha et al., 2010). Control synovial tissues were obtained from 10 patients who underwent arthroscopic surgery for severe joint trauma and had no other joint abnormalities or systemic diseases.

### Reverse transcription-quantitative polymerase chain reaction (RT-qPCR)

Total RNA was extracted from cells and tissues using TRIGene Reagent (GenStar BioSolutions, China), and first-strand cDNA was synthesized using the extracted total RNA as a template and a PrimeScript™ RT Reagent Kit (Takara Biotechnology, China). qPCR analysis was conducted using the FastStart Universal SYBR Green Master (Roche Applied Science, Germany) on an ABI7500 real-time fluorescence qPCR instrument. The $2^{-\Delta\Delta Ct}$ method was used for normalization to glyceraldehyde-3-phosphate dehydrogenase (*GAPDH*). The primers used for RT-qPCR were as follows: *LRRC15* forward primer: 5′-CGTTGCTGTTCCAAGCGTCCAT-3′, reverse primer: 5′-GCTCAGTGGTAGAAGAGACGGA-3′; *RUNX1* forward primer: 5′-CCACCTACCACAGAGCCATCAA-3′, reverse primer: 5′-TTCACTGAGCCGCTCGGAAAAG-3′; *GAPDH* forward primer: 5′-GTCTCCTCTGACTTCAACAGCG-3′, reverse primer: 5′-ACCACCCTGTTGCTGTAGCCAA-3′.

### Protein preparation and western blot assay

Total protein was extracted from cells using RIPA Lysis Buffer (Phygene, China) and quantified using the BCA Protein Assay Kit (Phygene). Proteins were separated using 12% SDS-PAGE and transferred to PVDF membranes. The membranes were blocked with 5% bovine serum albumin for 2 h at room temperature and incubated overnight at 4°C with primary antibodies against LRRC15 (1:1,000, ab150376; Abcam, UK), RUNX1 (1:1,000, PA5-85543; Thermo Fisher Scientific, USA), CBF-β (1:1,000, ab231345; Abcam), and GAPDH (1:2,000, #5174; Cell Signaling Technologies, USA). After that, the membranes were further incubated with horseradish peroxidase (HRP)-coupled secondary IgG antibody (1:10,000, ab6721; Abcam) for 120 min at room temperature. Protein bands were examined using an ECL substrate kit (Abcam), and all proteins were quantified based on the internal reference band GAPDH using ImageJ software.

### Isolation and culture of FLS

Synovial tissues from RA patients and normal controls were dissected, rinsed 2-3 times with phosphate-buffered saline (PBS), and minced into approximately 1 $mm^3$ pieces. Tissue fragments were transferred to flasks containing Dulbecco's modified Eagle's medium (Gibco, USA) supplemented with 10% fetal bovine serum (FBS) and incubated at 37°C in a 5% $CO_2$ incubator. When the cells reached confluence (5-7 days), they were passaged. Cells were considered FLS when a typical spindle-shaped, fibroblast-like appearance was present and the positive rate for the surface marker CD90 (Manferdini et al., 2016; Zhang et al., 2021) was >90%. FLS at passages 3-6 were used for subsequent experiments.

### RNA interference assay

The DNA overexpression plasmids oe-RUNX1 and oe-CBF-β based on pEXP-RB-Mam vector and a control plasmid were purchased from Guangzhou RiboBio (China). Short hairpin RNA (shRNA) targeting *LRRC15* (sh-*LRRC15* 1#, 2#, and 3#, based on mammalian shRNA interference piggyBac vector shRNA) and a negative control sh-NC were purchased from VectorBuilder (China). The sequences of shRNAs were as follows: sh-*LRRC15* 1#: 5′-CGAAGTGTAACGGAATCTAGTGTCTTTCTAATGTGGTAAAA-3′; sh-*LRRC15* 2#: 5′-TCCTTCCGCCCCAGGTTTCTTCTTCTCTTAAGGAGAGATTG-3′; sh-*LRRC15* 3#: 5′-TGATTCTTAGCCGCAATCAGATCAGCTTCATCTCCCCGGGT-3′. All transfections were performed using Lipofectamine 2000 (Thermo Fisher Scientific) according to the manufacturer's protocol. The cells were treated with 5 μM RO5-3335 (HY-108470; MedChemExpress, USA) or dimethyl sulfoxide (DMSO) for 24 h.

### Proliferation assay by cell counting kit (CCK)-8

CCK8 kits (GlpBio, USA) were used to assess the proliferative capacity of RA-FLS. The cells were plated in 96-well plates at $1 \times 10^3$ cells/well, and the plates were pre-incubated in a humidified incubator for designated times (0, 24, 48, and 72 h). Next, 10 μl of CCK8 solution was added to each well of the plate, and the plates were incubated for 2 h. Cell proliferation was determined by measuring the optical density at 450 nm using a microplate reader.

### DNA synthesis assay by EdU assay

The BeyoClick™ EdU-594 Cell Proliferation Assay Kit (Beyotime Biotechnology, China) was used to detect DNA synthesis by RA-FLS. The cells were plated in 96-well plates at $1 \times 10^5$ cells/well and incubated for 120 min at room temperature with a 20 μM EdU working solution. The cells were fixed with 4% neutral paraformaldehyde and treated with 0.5% Triton X-100 and Click-iT reaction mixture for 0.5 h at room temperature in the dark. The cells were then stained with 5 μg/ml Hoechst 33342 for 15 min at room temperature in the dark, and staining was detected by confocal microscopy (Carl Zeiss, Germany).

### Cell migration and invasion assays using Transwells®

HTS Transwell®-96 Permeable Support with an 8.0 μm Pore Polyester Membrane (Corning Glass Works, USA) was used to evaluate the migration and invasion of RA-FLS. When used for invasion assays, the membranes were precoated with Ceturegel™ Matrix LDEV-Free Matrigel (Yeasen Biotechnology, China). RA-FLS ($1 \times 10^5$) were resuspended in serum-free medium and placed in the apical chamber of the Transwell, and the basolateral chamber was supplemented with medium containing 10% FBS. After 24 h of normal culture, cells on the upper surface of the membrane were wiped off, and the cells that migrated or invaded the lower surface of the membrane were fixed with 4% neutral paraformaldehyde and stained with crystal violet. The number of cells was observed under a microscope (Olympus Optical, Japan) to measure their ability to migrate and invade.

### Angiogenesis assay of human umbilical vascular endothlial cells (HUVECs)

HUVECs ($1 \times 10^4$ cells/well; ATCC, USA) were seeded in 96-well plates coated with Ceturegel™ Matrix LDEV-free Matrigel and incubated at 37°C for 1 h. The supernatant of RA-FLS after different treatments was added to the culture wells of HUVECs as conditioned medium. The 96-well plates were incubated for 6 h and photographed under an inverted microscope for tube formation visualization. Tube-forming capability was quantified by counting the total number of closed polygons formed.

### Cytokine measurements

Pro-inflammatory cytokine concentrations in RA-FLS were measured using human interleukin (IL)-6 (K4143) and IL-1β (E4818) ELISA kits (BioVision, USA), according to the manufacturer's protocol. Concentrations of pro-inflammatory cytokines in mouse synovial tissues were measured using mouse IL-1β (ab197742; Abcam) and IL-6 (ab222503; Abcam) kits.

### Model establishment and treatment of mice

Thirty-five 8-week-old male DBA/1J mice were purchased from Beijing HFK Bioscience (China). The mice were fed a normal rodent diet and provided water *ad libitum* under a humidity (50%-60%) and climate (22°C)-controlled environment with a 12 h light-dark cycle. Animal experiments were performed following the ARRIVE guidelines and approved by the Animal Ethics Committee of Jinling Hospital, Jinling Clinical Medical College of Nanjing Medical University (approval No. 2022DZGKJDWLS-0020).

Thirty mice were induced with CIA, and the remaining five mice were injected with an equal volume of PBS as a control. In CIA mice, bovine type II collagen (CII; Chondrex, USA) was emulsified in an equal volume of complete Freund's adjuvant (Chondrex). Each mouse was intradermally injected at the tail root with 100 μl of an emulsion containing 100 μg of CII. Twenty-one days after the initial immunization, the mice received a booster injection of 100 μg CII emulsified with an equal volume of incomplete Freund's adjuvant (Chondrex). After the second immunization of CIA mice (day 21), 30 mice were divided into the following six groups (n = 5 each): CIA, adeno-associated viruses (AAV)-NC, AAV-shLRRC15, AAV-RUNX1, AAV-RUNX1 + AAV-LRRC15, and AAV-RUNX1 + RO5-3335 groups.

The AAV used in animal experiments was purchased from VectorBuilder and had a virus titer of $2 \times 10^{11}$ GC/ml. After the second immunization of CIA mice (day 21), each mouse subjected to AAV treatment was administered 50 μl of each AAV through the tail vein. Mice undergoing RO5-3335 treatment were administered 300 mg/kg/day RO5-3335 for 30 days starting on day 21.

The severity of arthritis was scored every seven days from day 21 to day 56. Arthritis was monitored using the Arthritis Index scoring system described as follows (Bevaart et al., 2010): 0, normal; 1, swelling of one joint (wrist/ankle or digit); 2, swelling of > two joints; 3, swelling of all joints; and 4, swelling of all joints and ankylosis. A maximum score of 4 was reached per paw, resulting in a maximum score of 16 per mouse. At the end of the experiment (day 56), all mice were euthanized by sodium pentobarbital overdose (150 mg/kg, intraperitoneally), and bone, joint, and synovial tissues were harvested.

### Histologic staining

The tissues were fixed in 4% paraformaldehyde and embedded in paraffin. Then, 5-μm sections were cut using a microtome (Leica Microsystems, Germany), dewaxed, dehydrated, and subjected to antigen retrieval. Subsequently, endogenous peroxidase was removed using 3% $H_2O_2$, and the tissue sections were incubated overnight at 4°C with primary antibodies against LRRC15 (1:200, M041540; Abmart Shanghai, China), CBF-β (1:200, ab231345; Abcam), and RUNX1 (1:1,000, PA5-85543; Thermo Fisher Scientific). The sections were incubated with HRP-coupled secondary IgG antibody (1:2,000, ab6721; Abcam) for 60 min at room temperature and stained with DAB reagent. After counterstaining with hematoxylin, the sections were photographed under a microscope and the tan-positive stained areas of each section were analyzed using ImageJ.

For H&E and Safranin O-fast green staining, paraffin-embedded sections were dewaxed, sequentially dehydrated, and stained using standard protocols (Beijing Solarbio Life Sciences, China). Finally, photographs were obtained under a light microscope to analyze pathological changes involving the mouse tissues.

### Chromatin immunoprecipitation (ChIP)

The ability of RUNX1 to enrich the *LRRC15* promoter was assayed using a Pierce™ Agarose ChIP kit (Thermo Fisher Scientific). Briefly, RA-FLS were cross-linked with 1% paraformaldehyde at room temperature for 10 min, then 0.125 M glycine was added to arrest the crosslinking reaction. The cells were centrifuged, lysed with a buffer containing Protease Inhibitor Cocktail, and centrifuged again to obtain nuclei. An ultrasonic disruptor was set to 4 s per ultrasonic cycle at 8-s intervals for 6 min. After addition of elution buffer containing RNase A, the samples were incubated with Proteinase K for 2 h at 62°C. Fragmented chromatin extracts were incubated with ChIP Grade RUNX1 antibody (1:50, ab272456; Abcam) or normal rabbit IgG (Thermo Fisher Scientific) overnight at 4°C, and with protein A/G magnetic beads for 2 h at 4°C. After thorough washing, elution, and de-crosslinking, purified DNA was used for qPCR analysis. PCR primer sequences for the *LRRC15* promoter were as follows: forward primer: 5′-TGCCTACTTACCAGCAGCTC-3′, reverse primer: 5′-GCCAGCTATGTGTACCCTGT-3′.

### Dual-luciferase reporter gene assay

The *LRRC15* promoter sequence bound by RUNX1 was obtained from Jaspar (https://jaspar.genereg.net/) and cloned upstream of the luciferase reporter gene of pGL3-Basic Luciferase Reporter Vector (Promega, USA). The constructs, oe-RUNX1, oe-NC, and pRL-TK plasmids were then co-transfected into RA-FLS using Lipofectamine 2000 and treated with or without RO5-3335 as needed. After 48 h, luciferase activity was measured using the Dual-Luciferase Reporter Assay System (Promega).

### Co-IP

Total protein in the cells was extracted using RIPA Lysis Buffer (Phygene) and centrifuged at 14,000 × *g* for 10 min at 4°C. The supernatant was transferred to a new centrifuge tube and served as the cell lysate. The supernatant (20 μl) was used as the input, and 200 μl of the supernatant was incubated for 2 h at 4°C with antibodies against RUNX1 (1:100, 19555-1-AP; ProteinTech Group, USA) or CBF-β (1:100, ab125191; Abcam) covalently attached to protein G agarose beads (Millipore, USA). Bound proteins were eluted with 100 mM NaCl and 15 mM Tris-HCl. The protein expression of RUNX1 and CBF-β in the input and IP groups was detected using western blotting.

### Statistics

Statistical analyses were performed using Prism 8.0 (Graphpad Software, USA). All results are presented as mean ± SD of at least three experiments. Statistical significance was determined using unpaired Student's *t*-tests for independent data. Multiple groups of samples were analyzed using one- or two-way ANOVA, and pairwise comparisons were adjusted using Tukey's method. Differences were considered statistically significant at $P < 0.05$.

## RESULTS

### LRRC15 is significantly overexpressed in RA patients

The dataset GSE77298, containing 16 microarrays of end-stage RA synovial biopsies and 7 microarrays of synovial biopsies from individuals without joint disease, was selected from the GEO database to screen for differentially expressed genes in RA (Fig. 1A). Among them, *LRRC15* (GPL570 annotation platform No. 213909_at) was the most significantly differentially expressed gene, and its expression was significantly elevated in RA (Fig. 1B). We then detected *LRRC15* expression in synovial tissues collected from patients with RA and normal synovial tissues using RT-qPCR and immunohistochemistry. Elevated expression was confirmed in the synovial tissues of our cohort (Figs. 1C and 1D).

### Knockdown of LRRC15 inhibits proliferation and inflammatory response of RA-FLS

We isolated FLS from synovial tissues of patients with RA and controls (named RA-FLS and Control-FLS therein). We detected a much higher expression of LRRC15 in RA-FLS than in Control-FLS using RT-qPCR and western blotting (Figs. 2A and 2B). Subsequently, we transfected three shRNAs of *LRRC15* into RA-FLS and detected their inhibition efficiency using RT-qPCR (Fig. 2C). We selected sh-*LRRC15* 2# with the best inhibition effect for subsequent experiments and termed it sh-*LRRC15*. Assaying the proliferative capacity of cells by CCK8 assays, we observed that sh-*LRRC15* significantly suppressed the proliferation of RA-FLS (Fig. 2D). A decrease in cellular DNA synthesis in the presence of sh-*LRRC15* was also observed using EdU staining (Fig. 2E). ELISA results revealed that inhibition of LRRC15 reduced the levels of IL-6 and IL-1β in RA-FLS (Fig. 2F).

### Knockdown of LRRC15 inhibits migration, invasion, and angiogenesis of RA-FLS

Remarkably, we observed a reduction in the migratory and invasive abilities of RA-FLS in the presence of sh-*LRRC15* in Transwell assays (Figs. 3A and 3B). The culture medium of RA-FLS was collected as conditioned medium, and using angiogenesis assays, we found that blocking of LRRC15 also inhibited the angiogenic ability of RA-FLS (Fig. 3C).

### LRRC15 knockdown ameliorates joint damage in CIA mice

RA mouse models were induced by CIA, and our preliminary experiments confirmed that an AAV titer of $2 \times 10^{11}$ GC/ml was able to successfully infect the lung, liver, and synovial tissues of mice after 30 days (Supplementary Fig. S1). CIA mice were treated with AAV-shLRRC15 or AAV-NC (Fig. 4A). We observed a significant increase in the arthritis score in CIA mice compared to that in control mice, while AAV-shLRRC15 treatment reduced the arthritis score in CIA mice (Fig. 4B). The synovial tissues of CIA mice exhibited significantly enhanced expression of LRRC15, whereas AAV-shLRRC15 treatment decreased LRRC15 expression in the synovial tis-

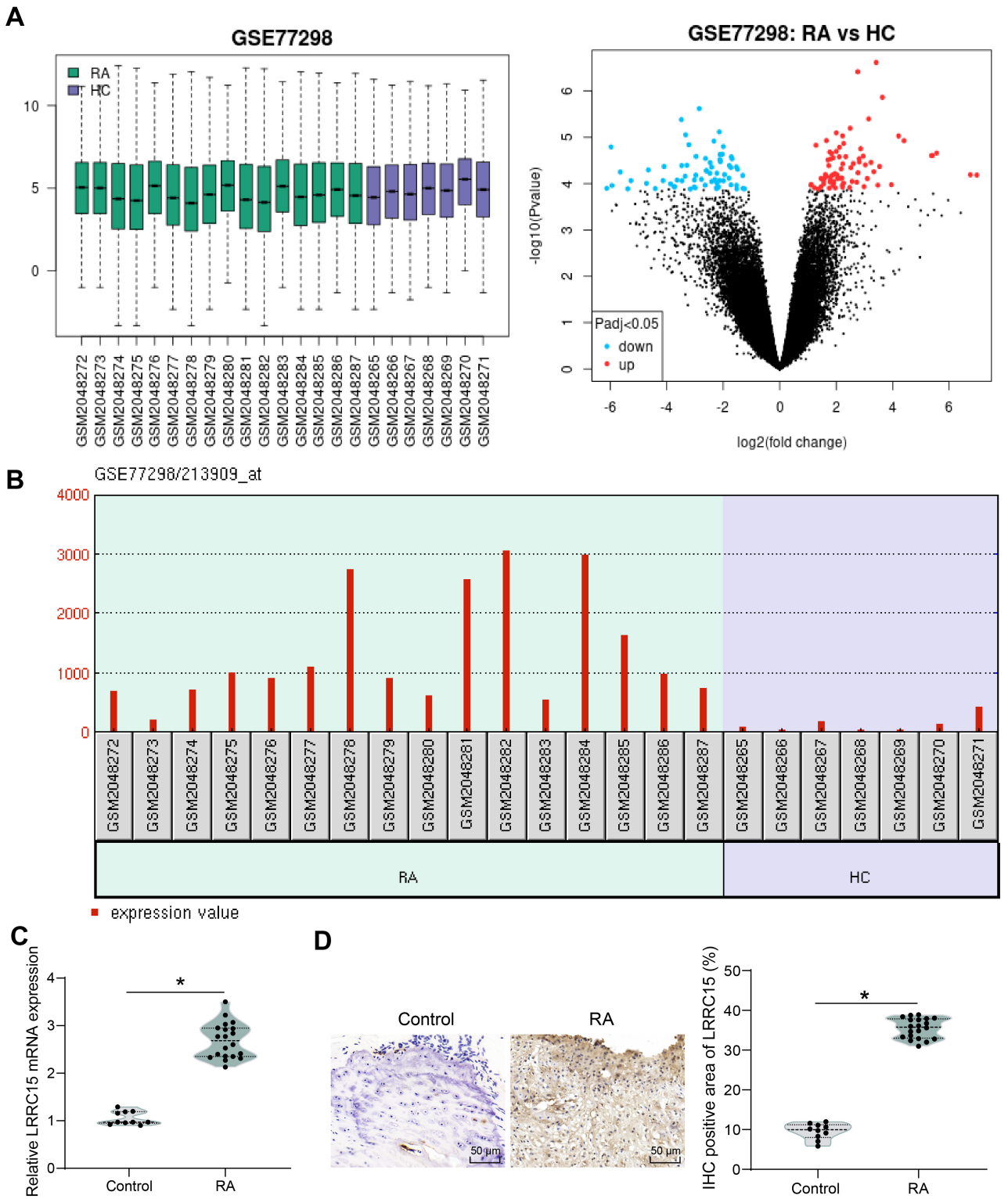


**Fig. 1. Expression of LRRC15 is upregulated in human RA synovial tissues.** (A) Gene Expression Omnibus (GEO) database screening for differentially expressed genes in RA synovial tissues. (B) Expression of LRRC15 in the GEO database. Expression of LRRC15 in collected synovial tissues of RA patients (n = 20) and normal controls (n = 10) by RT-qPCR (C) and immunohistochemistry (IHC) (D). Data are presented as mean ± SD. Statistical significance was determined using unpaired *t*-tests for independent data. $*P < 0.05$ vs control group. LRRC15, leucine-rich repeat containing 15; RA, rheumatoid arthritis; HC, healthy controls.

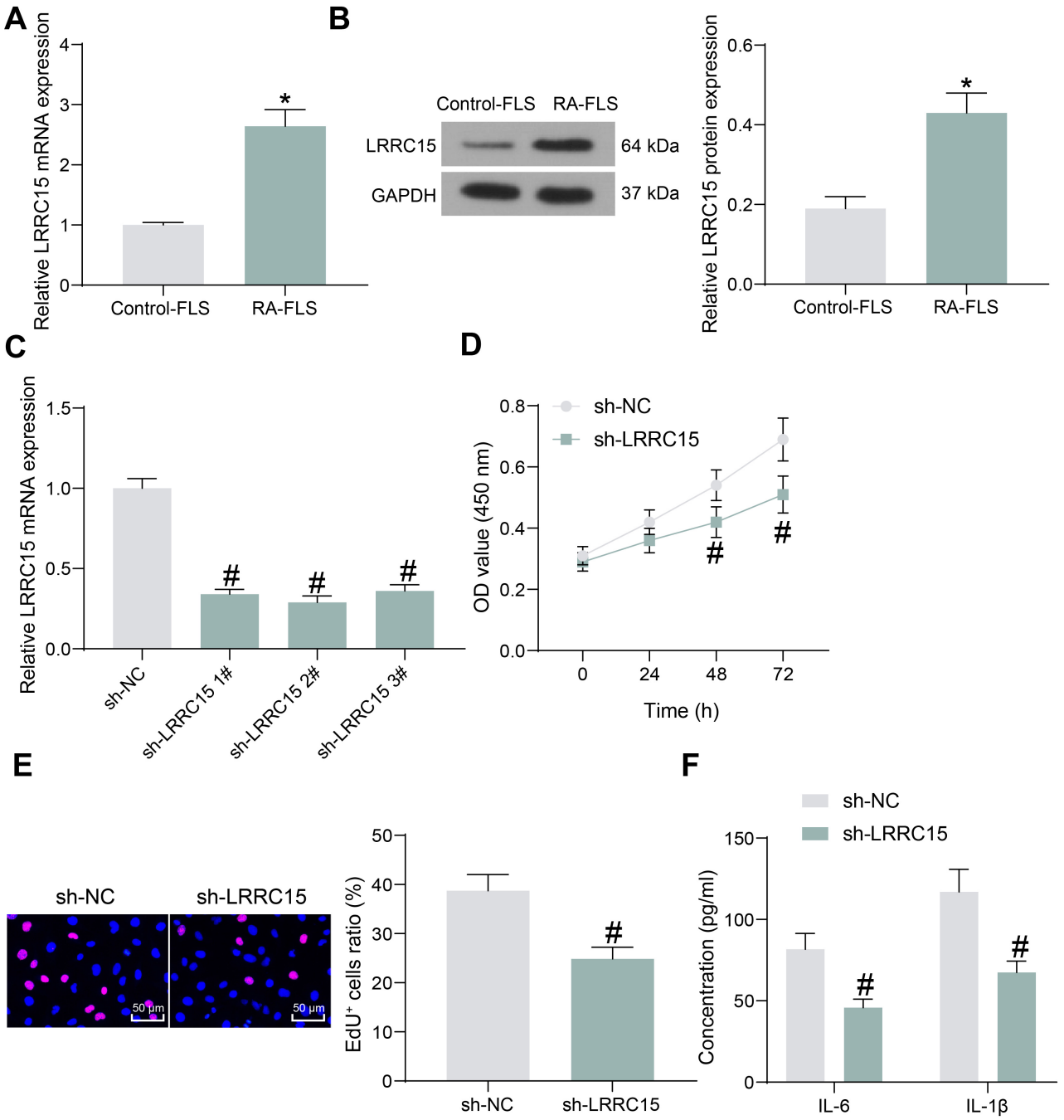


**Fig. 2. Depletion of LRRC15 protects RA-FLS from proliferation and inflammation.** Detection of LRRC15 expression in RA-FLS and Control-FLS by RT-qPCR (A) and western blot (B). (C) The inhibition efficiency of shRNAs of LRRC15 by RT-qPCR. (D) The proliferative capacity of RA-FLS by CCK8 assay. (E) The DNA synthesis of RA-FLS by EdU staining. (F) Pro-inflammatory cytokine concentrations in RA-FLS by ELISA. Data are presented as mean ± SD of the mean of at least 3 independent experiments. Statistical significance was determined using unpaired *t*-tests for independent data. Multiple groups of samples were analyzed by one-way or two-way ANOVA, and pairwise comparisons were adjusted by Tukey's method. $^{*}P < 0.05$ vs Control-FLS. $^{\#}P < 0.05$ vs sh-NC. LRRC15, leucine-rich repeat containing 15; RA-FLS, rheumatoid arthritis-associated fibroblast-like synoviocytes; OD, optical density; NC, negative control.

sues of mice, as evidenced by immunohistochemistry (Fig. 4C). Elevated levels of IL-6 and IL-1β in the synovial tissues of CIA mice were detected by ELISA, whereas the levels of these pro-inflammatory cytokines were significantly reduced after inhibition of LRRC15 (Fig. 4D). H&E staining of CIA mice showed pathological changes, including synovial hyperplasia and pannus formation, which were alleviated by inhibition of LRRC15 (Fig. 4E). We found that CIA mice exhibited erosion

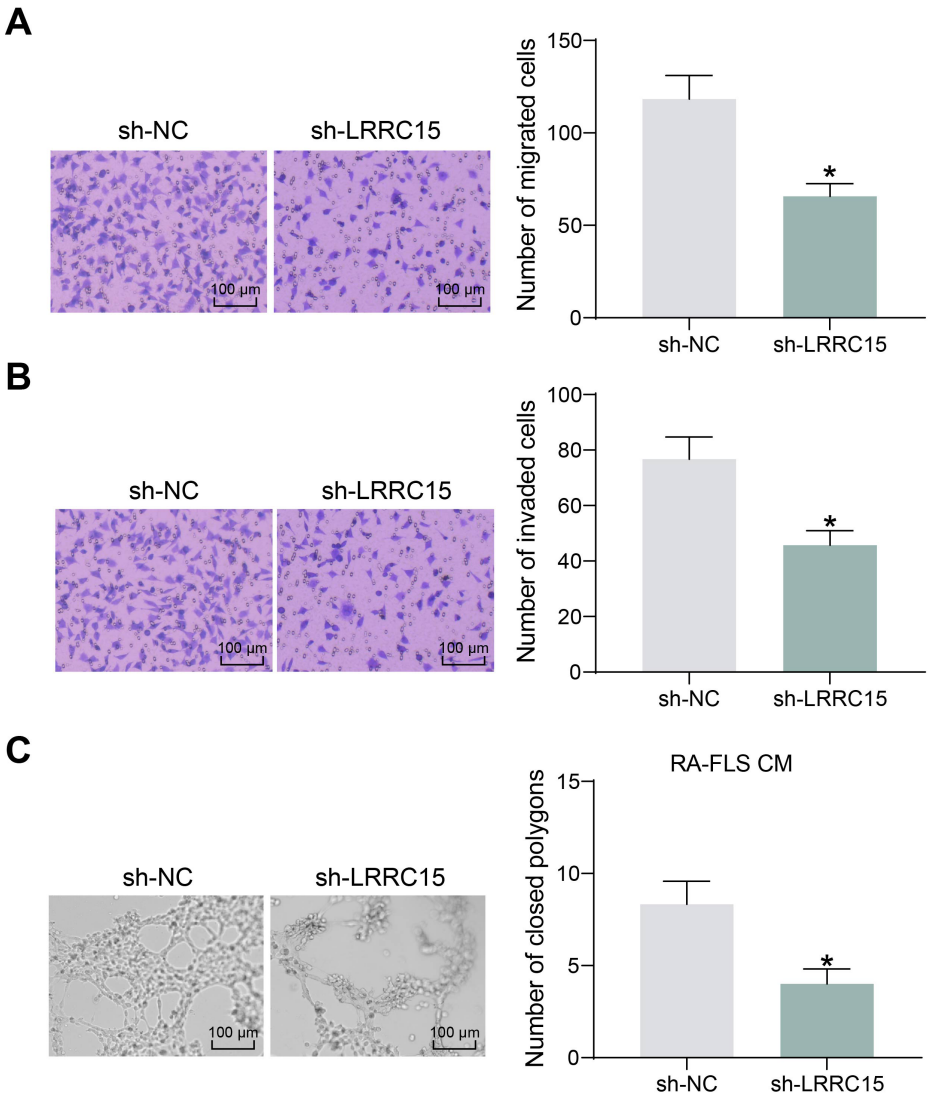


**Fig. 3. Depletion of LRRC15 inhibits RA-FLS migration, invasion, and angiogenesis.** (A) RA-FLS migration by Transwell assay. (B) RA-FLS invasion by Transwell assay. (C) Angiogenic capacity of RA-FLS by angiogenesis assay. Data are presented as mean ± SD of the mean of at least 3 independent experiments. Statistical significance was determined using unpaired *t*-tests for independent data. $*P < 0.05$ vs sh-NC. LRRC15, leucine-rich repeat containing 15; RA-FLS, rheumatoid arthritis-associated fibroblast-like synoviocytes; NC, negative control.

and destruction of articular bone and cartilage by staining with Safranin O-fast green, and loss of LRRC15 ameliorated such pathological changes in tissues (Fig. 4F).

## RUNX1-CBF-β interaction represses LRRC15 transcription

To investigate the causes of LRRC15 overexpression in RA synovial tissues, we screened for upstream transcription factors responsible for the regulation of LRRC15 in hTFtarget (http://bioinfo.life.hust.edu.cn/hTFtarget/#!/) and performed pathway enrichment analysis (Fig. 5A). Among the top-three enriched pathways, there was only one intersection, RUNX1 (Fig. 5B).

In the GSE77298 dataset, RUNX1 (GPL570 annotation platform No. 1563591_at) expression was downregulated in RA synovial tissues, but the difference was not statistically significant (Fig. 5C). We speculated that individual differences in patients with RA resulted in the generation of two extreme points that deviated far from the mean. Poor expression of RUNX1 was also determined in RA-FLS by RT-qPCR and western blotting (Figs. 5D and 5E). Using the ChIP-seq database Cistrome Data Browser (http://cistrome.org/db/#/), we found that there was a binding peak between RUNX1 and the *LRRC15* promoter region (Fig. 5F), and the enrichment ability of RUNX1 to the *LRRC15* promoter was directly demonstrated by ChIP-qPCR experiments (Fig. 5G).

An overexpression DNA plasmid of *RUNX1* was transfected into RA-FLS, followed by treatment with RO5-3335 to impair interactions between RUNX1 and CBF-β (DMSO as a control). The expression of related proteins was measured using western blotting (Fig. 5H). RUNX1 overexpression significantly inhibited LRRC15 expression. Upon further RO5-3335 treatment, the expression of RUNX1 remained unchanged, while the expression of LRRC15 was significantly rescued. No significant variations were observed in the expression of CBF-β after overexpression of RUNX1 or RO5-3335.

Further immunohistochemical staining and western blotting showed that CBF-β was slightly upregulated in RA synovial tissues and RA-FLS (Supplementary Figs. S2A and S2B). We upregulated CBF-β in RA-FLS by transfection with DNA overexpression plasmids, and we observed a decrease

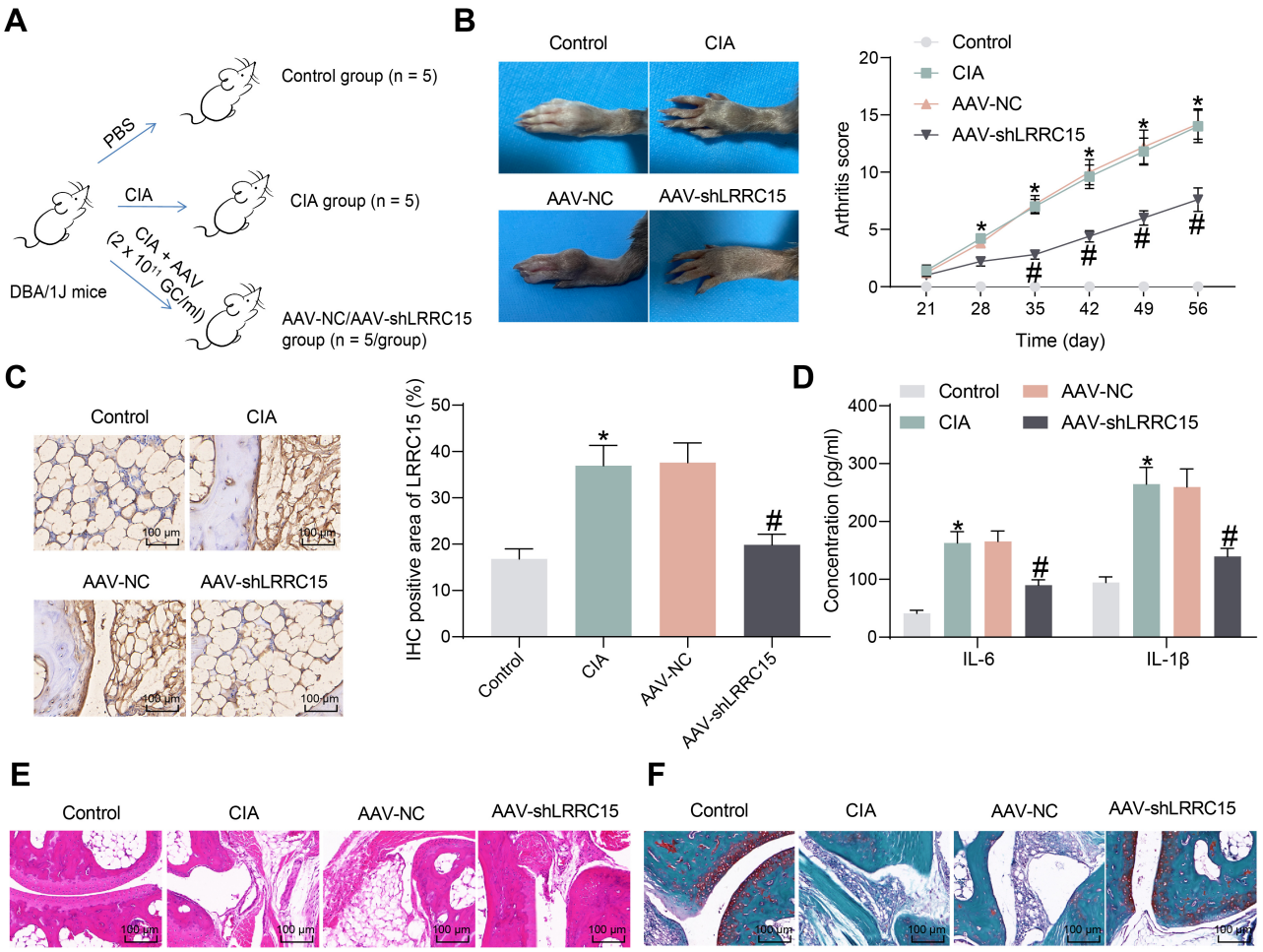


**Fig. 4. Depletion of LRRC15 alleviates CIA in mice.** (A) The flow chart of mouse treatment: DBA/1J mice induced with CIA (phosphate-buffered saline [PBS] as control) were further administrated with AAV-shLRRC15 or AAV-NC ($2 \times 10^{11}$ GC/ml). (B) Arthritis scores of each group of mice and representative images of the joints of mice on day 56. (C) Immunohistochemical (IHC) staining of LRRC15 expression in mouse synovial tissues. (D) Detection of IL-6, IL-1β in mouse synovial tissues by ELISA. (E) Detection of pathological changes in mouse synovial tissues by H&E staining. (F) Erosion and destruction of bone tissues in mice detected by Safranin O-fast green staining. Data are presented as mean ± SD (n = 5). Multiple groups of samples were analyzed by one-way or two-way ANOVA, and pairwise comparisons were adjusted by Tukey's method. $^{*}P < 0.05$ vs Control. $^{\#}P < 0.05$ vs AAV-NC. LRRC15, leucine-rich repeat containing 15; CIA, collagen-induced arthritis; AAV, adeno-associated viruses; NC, negative control; IL, interleukin.

in LRRC15 expression upon overexpression of CBF-β using RT-qPCR and western blotting, indicating that CBF-β regulation can also affect LRRC15 expression (Supplementary Figs. S2C and S2D). Decreased protein content in immunoprecipitation experiments was detected using a Co-IP assay, indicating diminished interactions between RUNX1 and CBF-β in RA-FLS relative to Control-FLS (Supplementary Fig. S2E). It is worth noting that, considering the basal expression of RUNX1 and CBF-β in RA (only RUNX1 expression was significantly reduced in RA), the elevated LRRC15 expression and reduced interaction between RUNX1 and CBF-β in RA were mainly affected by the downregulation of RUNX1. The direct binding site of RUNX1 on the *LRRC15* promoter was obtained from Jaspar (https://jaspar.genereg.net/) (Fig. 5I). The results of dual-luciferase reporter gene assays showed that overexpression of RUNX1 significantly repressed the transcriptional activity of the *LRRC15* promoter, whereas RO5-3335 treatment partially restored the transcription of *LRRC15* (Fig. 5J).

## RUNX1-CBFβ-mediated inhibition of LRRC15 regulates phenotypic changes in RA-FLS

We transfected the overexpression DNA plasmid of *LRRC15* into RA-FLS overexpressing RUNX1 and confirmed the overexpression efficiency using RT-qPCR (Fig. 6A). By detecting changes in cell proliferation using CCK8 assays, we observed that RUNX1 overexpression significantly inhibited the proliferation of RA-FLS. Conversely, the anti-proliferative properties of RUNX1 on RA-FLS were compromised after blocking RUNX1-CBF-β interactions by RO5-3335 or overexpression

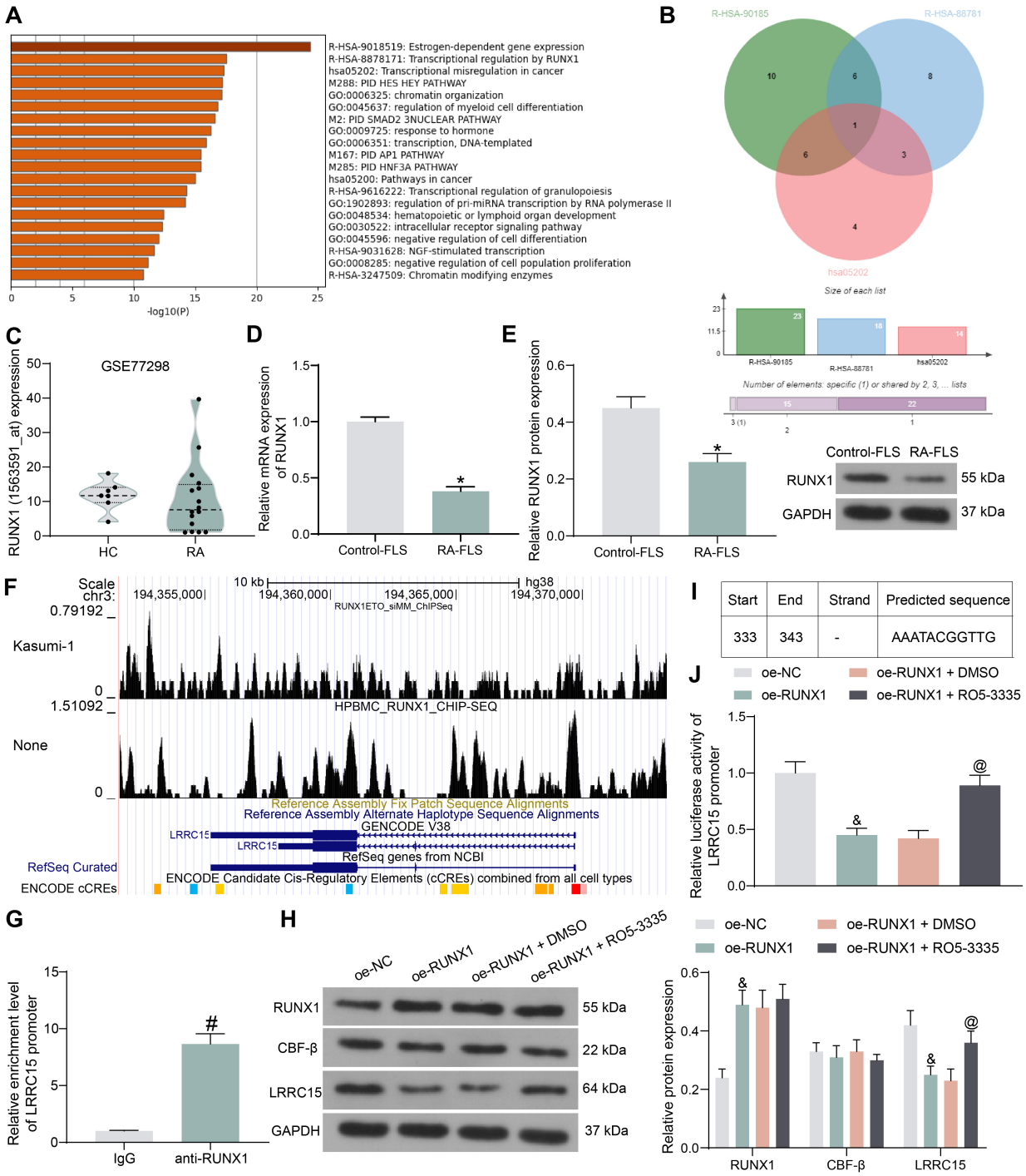


**Fig. 5. Epigenetic suppression of LRRC15 by RUNX1 is identified in RA-FLS.** (A) Pathway enrichment analysis of transcription factors that transcriptionally regulate LRRC15. (B) Intersecting genes in the enriched pathways. (C) RUNX1 expression in the GSE77298 dataset. Detection of RUNX1 expression in RA-FLS by RT-qPCR (D) and western blot (E). (F) Binding relationship of RUNX1 to LRRC15 promoter predicted in the Cistrome Data Browser. (G) The enrichment ability of RUNX1 on LRRC15 promoter by ChIP-qPCR. (H) RUNX1, CBF-β, and LRRC15 protein expression in RA-FLS in response to oe-RUNX1 or oe-RUNX1 + RO5-3335 by western blot. (I) Binding site of RUNX1 on LRRC15 promoter predicted in Jaspar. (J) The regulatory effect of RUNX1 on the transcriptional activity of LRRC15 promoter by dual-luciferase reporter assays. Data are presented as mean ± SD of at least 3 independent experiments. Statistical significance was determined using unpaired *t*-tests for independent data. Multiple groups of samples were analyzed by one-way or two-way ANOVA, and pairwise comparisons were adjusted by Tukey's method. $*P < 0.05$ vs Control-FLS. $^{\#}P < 0.05$ vs IgG. $^{\&}P < 0.05$ vs oe-NC. $^{@}P < 0.05$ vs oe-RUNX1 + DMSO. LRRC15, leucine-rich repeat containing 15; RUNX1, runt-related transcription factor 1; RA-FLS, rheumatoid arthritis-associated fibroblast-like synoviocytes; HC, healthy controls; CBF-β, core-binding factor subunit beta; NC, negative control; DMSO, dimethyl sulfoxide.

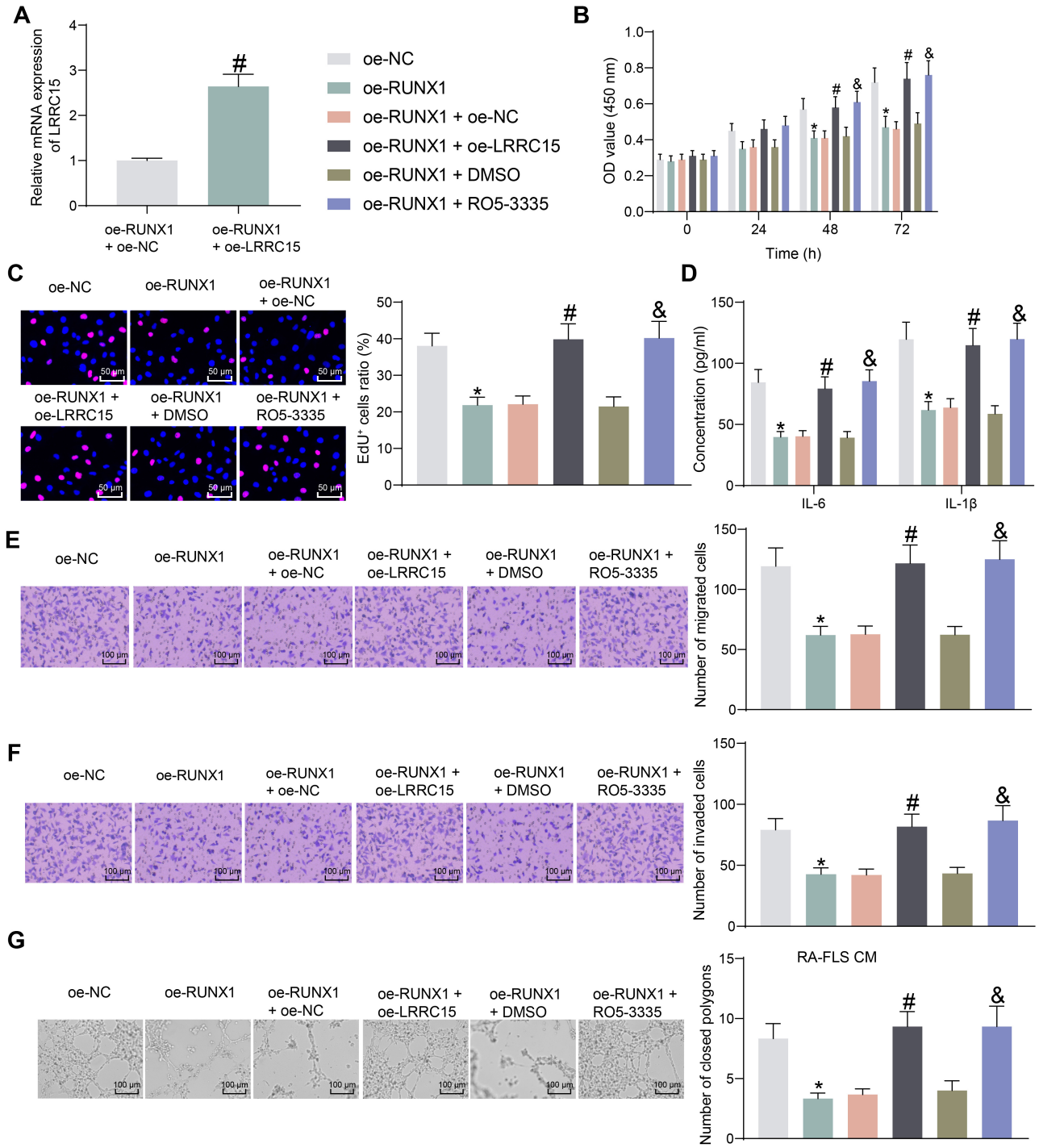


**Fig. 6. RUNX1-CBF-β-mediated inhibition of LRRC15 leads to RA-FLS phenotypic changes.** (A) Overexpression efficiency of oe-LRRC15 by RT-qPCR. (B) The proliferative capacity of RA-FLS by CCK8 assay. (C) The DNA synthesis of RA-FLS by EdU staining. (D) Pro-inflammatory cytokine concentrations in RA-FLS by ELISA. (E) RA-FLS migration capacity by Transwell assay. (F) RA-FLS invasion capacity by Transwell assay. (G) Angiogenic capacity of RA-FLS by angiogenesis assay. Data are presented as mean ± SD of at least 3 independent experiments. Statistical significance was determined using unpaired *t*-tests for independent data. Multiple groups of samples were analyzed by one-way or two-way ANOVA, and pairwise comparisons were adjusted by Tukey's method. $^{*}P < 0.05$ vs oe-NC. $^{\#}P < 0.05$ vs oe-RUNX1 + oe-NC. $^{\&}P < 0.05$ vs oe-RUNX1 + DMSO. RUNX1, runt-related transcription factor 1; CBF-β, core-binding factor subunit beta; LRRC15, leucine-rich repeat containing 15; RA-FLS, rheumatoid arthritis-associated fibroblast-like synoviocytes; NC, negative control; DMSO, dimethyl sulfoxide; OD, optical density; IL, interleukin; CM, conditioned medium.

of LRRC15 (Fig. 6B). Similarly, the inhibitory effect of RUNX1 on DNA synthesis by RA-FLS was significantly reversed by RO5-3335 treatment or overexpression of LRRC15 (Fig. 6C). ELISA results showed that RUNX1 upregulation lowered the concentration of pro-inflammatory cytokines in cells, whereas RO5-3335 treatment or overexpression of LRRC15 accentuated the inflammatory response in RA-FLS (Fig. 6D). The migratory and invasive abilities of RA-FLS were also significantly inhibited upon overexpression of RUNX1, while RO5-3335 or oe-*LRRC15* rescued cell mobility (Figs. 6E and 6F). Finally, angiogenesis assays showed that RUNX1 also inhibited the angiogenic ability of RA-FLS, whereas blocking RUNX1-CBFβ interactions or overexpression of LRRC15 led to more pronounced tube formation in RA-FLS (Fig. 6G).

## RUNX1-CBFβ-mediated inhibition of LRRC15 ameliorates joint damage in CIA mice

CIA mice were further treated with AAV-RUNX1 in combina-

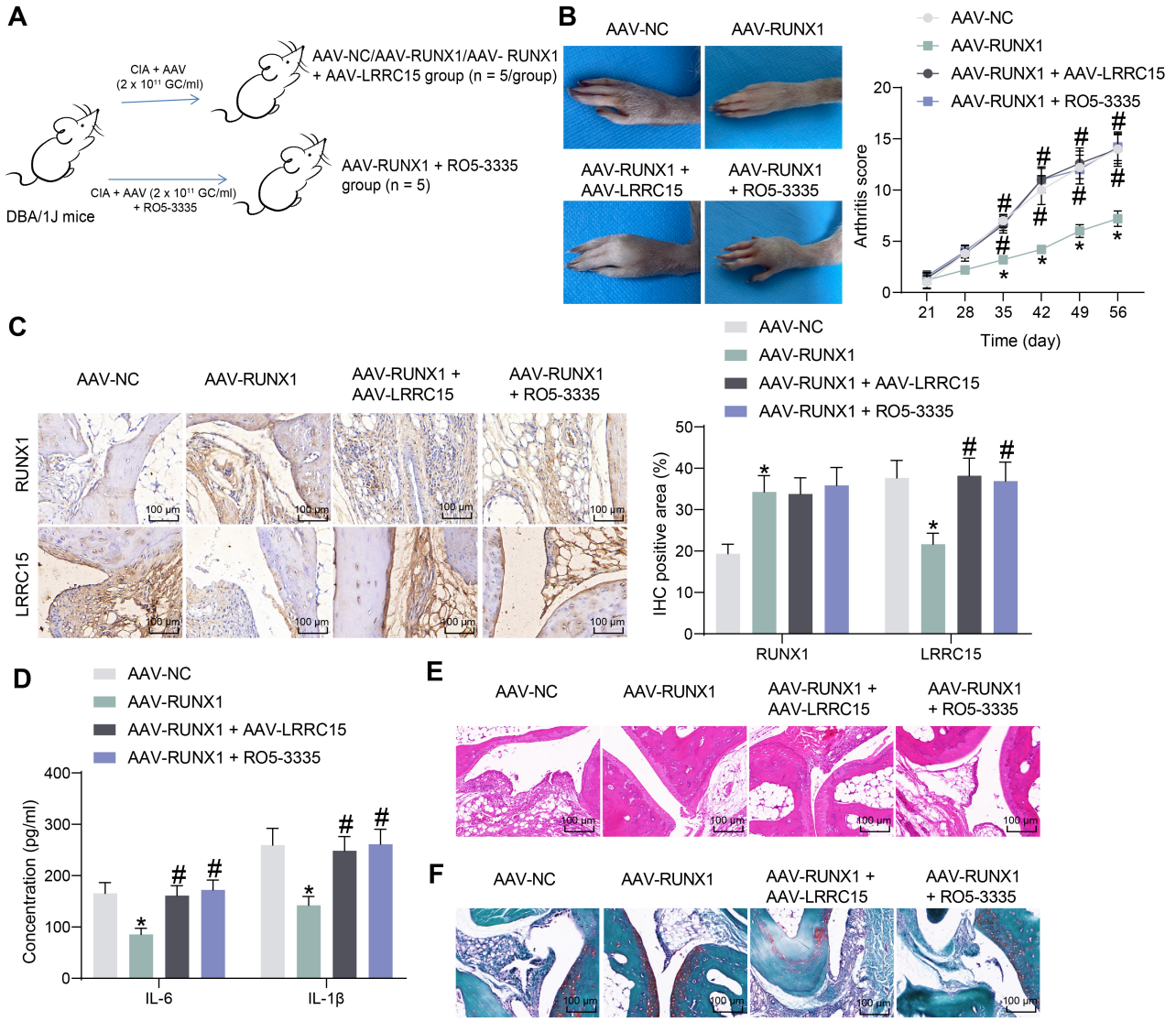


**Fig. 7. RUNX1-CBFβ-mediated inhibition of LRRC15 ameliorates joint damage in CIA mice.** (A) The flow chart of mouse treatment: CIA mice were further administrated with AAV-RUNX1 ($2 \times 10^{11}$ GC/ml), AAV-RUNX1 + AAV-LRRC15, or AAV-RUNX1 + RO5-3335. (B) Arthritis scores of each group of mice and representative images of the joints of mice on day 56. (C) Immunohistochemical (IHC) staining of RUNX1 and LRRC15 expression in mouse synovial tissues. (D) Detection of IL-6 and IL-1β in mouse synovial tissues by ELISA. (E) Detection of pathological changes in mouse synovial tissues by H&E staining. (F) Erosion and destruction of bone tissues in mice detected by Safranin O-fast green staining. Data are presented as mean ± SD (n = 5). Multiple groups of samples were analyzed by one-way or two-way ANOVA, and pairwise comparisons were adjusted by Tukey's method. $*P < 0.05$ vs AAV-NC. $^{\#}P < 0.05$ vs AAV-RUNX1. RUNX1, runt-related transcription factor 1; LRRC15, leucine-rich repeat containing 15; CIA, collagen-induced arthritis; AAV, adeno-associated viruses; NC, negative control; IL, interleukin.

tion with RO5-3335 or AAV-LRRC15 (Fig. 7A). We observed a significant decrease in arthritis scores in AAV-RUNX1 mice compared to that in AAC-NC mice, whereas the administration of RO5-3335 or AAV-LRRC15 resulted in increased arthritis scores in mice (Fig. 7B). The expression of RUNX1 and LRRC15 was detected using immunohistochemistry (Fig. 7C). A significant increase in RUNX1 expression and a significant decline in LRRC15 expression were observed in the synovial tissues of AAV-RUNX1-administrated mice. The application of RO5-3335 or AAV-LRRC15 did not affect RUNX1 expression but significantly increased LRRC15 expression in mouse synovial tissues. Overexpression of RUNX1 also decreased IL-6 and IL-1β levels in mouse synovial tissues as detected by ELISA, while RO5-3335 or AAV-LRRC15 treatment restored the levels of pro-inflammatory cytokines (Fig. 7D). H&E staining showed that the inhibitory effect of RUNX1 on synovial hyperplasia and pannus formation was significantly reversed by RO5-3335 or AAV-LRRC15 treatment (Fig. 7E). By staining with Safranin O-fast green, we found that RUNX1 ameliorated the erosion and destruction of articular bone and cartilage in mice, whereas RO5-3335 and AAV-LRRC15 reversed this protective effect of RUNX1 on bone tissues (Fig. 7F).

## DISCUSSION

LRRC15 is involved in cell-cell and cell-matrix interactions and has been recognized as a promising anti-cancer target because of its overexpression in mesenchymal-derived tumors and cancer-associated fibroblasts in breast, head and neck, lung, and pancreatic cancers (Ray et al., 2022). To elucidate potential regulators participating in the pathogenesis of RA, we screened the GEO database and found that LRRC15 levels were much higher in synovial tissues from RA patients than in normal controls. We demonstrated that LRRC15 deficiency suppressed RA-FLS proliferation and inflammation *in vitro* and pathological changes in CIA mice *in vivo*. Our study identified a new epigenetic modifier of LRRC15 and RUNX1 in RA through their interaction with CBF-β.

*LRRC15*, encoding a type I transmembrane protein, is a distinctly inducible gene that is responsive to β-amyloid and pro-inflammatory cytokines in astrocytes (Satoh et al., 2005). In addition, LRRC15 is a robust and emerging therapeutic target for cancer treatment (Cui et al., 2020). For instance, overexpression of LRRC15 in cancer-associated fibroblasts promotes cell migration and invasion in triple-negative breast cancer cells (Yang et al., 2022). According to Slemmons et al. (2021), LRRC15 antibody-drug conjugates exhibit promise as osteosarcoma therapeutics in preclinical studies. In addition, LRRC15 is upregulated in cartilage, synovial tissues, and subchondral bones of the medial region in osteoarthritic knees (Chen et al., 2018). Intriguingly, Galligan et al. (2007) found that LRRC15 is downregulated in the synovial tissues of patients with RA and osteoarthritis relative to that in controls. However, the microarray data they applied was U133Plus 2.0 oligonucleotide microarray GeneChip Arrays, which has recently been updated and might have caused such a discrepancy. Here, we confirmed the overexpression of *LRRC15* mRNA and protein in the synovial tissues of patients with RA and CIA mice. In addition, our observations showed that the knockdown of LRRC15 using shRNA not only constrained the aggressive phenotype of RA-FLS *in vitro*, but also played an anti-inflammatory role in CIA mice *in vivo*. Currently available biological agents and inhibitor therapies that target IL-1β and IL-6 cannot expedite complete patient remission and are unable to cure RA (Ganesan and Rasool, 2017). Furthermore, pannus development has been noted to be central to joint destruction, but why it develops in RA is unknown, and the molecular basis of pannus formation and the pathways by which FLS achieve and maintain an aggressive phenotype are not fundamentally understood (You et al., 2018). Im-

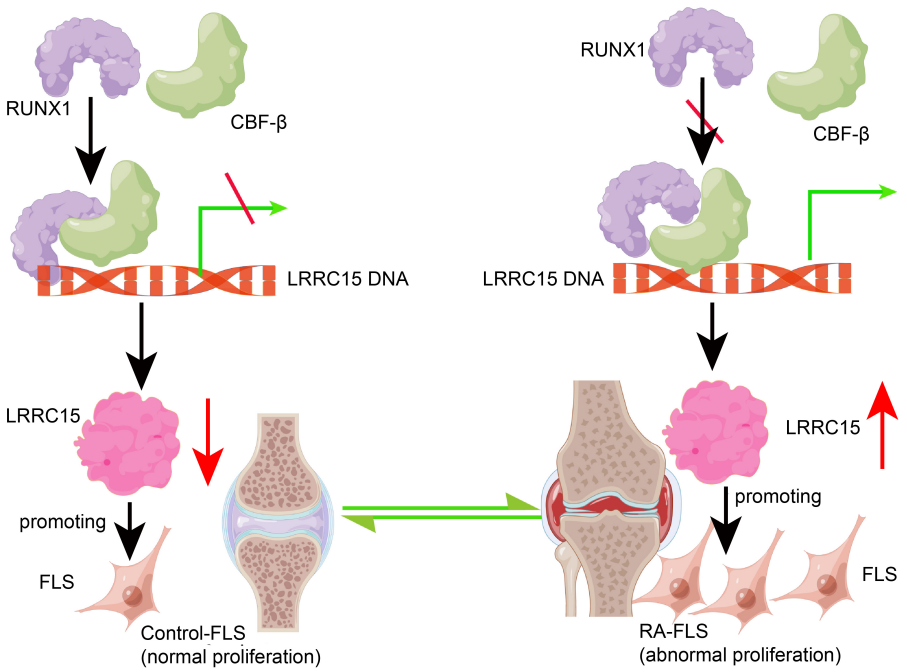


**Fig. 8. Schematic representation of LRRC15 involvement in RA pathogenesis.** RUNX1 represses the transcriptional expression of LRRC15 by binding to CBF-β, thereby inhibiting the FLS proliferation and ameliorating joint damage in RA. LRRC15, leucine-rich repeat containing 15; RA, rheumatoid arthritis; RUNX1, runt-related transcription factor 1; CBF-β, core-binding factor subunit beta; FLS, fibroblast-like synoviocytes. Plotted by Figdraw (https://www.figdraw.com/).

ages acquired after H&E and Safranin O-fast green staining demonstrated that depletion of LRRC15 can delay pannus formation and joint destruction. Therefore, our *in vitro* and *in vivo* evidence suggests that LRRC15 ablation may represent a potential therapeutic target for RA patients in the future.

Classically, epigenetic mechanisms describe chemical modifications of the histone tails or directly of DNA, thereby determining which genes in a cell are expressed or silenced (Ospelt et al., 2017). Dysregulation of transcription factors and co-factors may lead to bone deformities and bone mass disorders, and understanding the mechanisms involved in the modulation of these factors may provide solutions for treating bone diseases (Chan et al., 2021). To dissect the upstream mechanism of LRRC15 overexpression in RA, we conducted a series of bioinformatic predictions. It was thus identified that RUNX1 directly binds to the *LRRC15* promoter. RUNX1 mediates the transcription of genes by interacting with its partner, CBF-β (de Bruijn and Speck, 2004). RO5-3335 directly interacts with RUNX1 and CBFβ and represses RUNX1/CBF-β-dependent transactivation (Cunningham et al., 2012). In the present study, we found that RO5-3335 treatment significantly promoted the expression of LRRC15 in the presence of oe-*RUNX1*, without altering the expression of RUNX1, indicating that the expression of LRRC15 was indeed regulated by the RUNX1/CBF-β complex. According to van Hamburg and Tas (2018), proteins encoded by established genetic risk factors for RA, including RUNX1, are directly involved in T-helper 17 cell differentiation and/or function. More importantly, RUNX1 single-nucleotide polymorphisms are related to immunologic and autoimmune diseases, including RA (Korinfskaya et al., 2021). Here, we found that overexpression of RUNX1 repressed the proliferation and inflammatory response of RA-FLS, which was reversed by overexpression of LRRC15 or RO5-3335, indicating that LRRC15 is a putative downstream factor of RUNX1 in RA.

In summary, our study convincingly demonstrated that LRRC15 loss, mediated by the RUNX1/CBF-β complex, can ameliorate RA by reducing the aggressiveness of FLS, inducing pro-inflammatory cytokine secretion, synovial hyperplasia, angiogenesis, cartilage erosion, and bone destruction (Fig. 8). Further investigations are required to determine the downstream effectors of LRRC15 in RA.

*Note: Supplementary information is available on the Molecules and Cells website (www.molcells.org).*

## AUTHOR CONTRIBUTIONS

H.D., X.M., and J.Z. conceived and performed experiments, wrote the manuscript, and secured funding. P.F. and L.L. performed experiments. T.G. provided expertise and feedback.

## CONFLICT OF INTEREST

The authors have no potential conflicts of interest to disclose.

## ORCID

Hao Ding https://orcid.org/0000-0003-2688-3852
Xiaoliang Mei https://orcid.org/0000-0002-3576-0419
Lintao Li https://orcid.org/0000-0002-1298-2561
Peng Fang https://orcid.org/0000-0002-8684-2756
Ting Guo https://orcid.org/0000-0002-7815-9033
Jianning Zhao https://orcid.org/0000-0003-3950-9974

## REFERENCES

Ai, R., Laragione, T., Hammaker, D., Boyle, D.L., Wildberg, A., Maeshima, K., Palescandolo, E., Krishna, V., Pocalyko, D., Whitaker, J.W., et al. (2018). Comprehensive epigenetic landscape of rheumatoid arthritis fibroblast-like synoviocytes. Nat. Commun. *9*, 1921.

Alabarse, P.V.G., Lora, P.S., Silva, J.M.S., Santo, R.C.E., Freitas, E.C., de Oliveira, M.S., Almeida, A.S., Immig, M., Teixeira, V.O.N., Filippin, L.I., et al. (2018). Collagen-induced arthritis as an animal model of rheumatoid cachexia. J. Cachexia Sarcopenia Muscle *9*, 603-612.

Aletaha, D., Neogi, T., Silman, A.J., Funovits, J., Felson, D.T., Bingham, C.O., 3rd, Birnbaum, N.S., Burmester, G.R., Bykerk, V.P., Cohen, M.D., et al. (2010). 2010 rheumatoid arthritis classification criteria: an American College of Rheumatology/European League Against Rheumatism collaborative initiative. Ann. Rheum. Dis. *69*, 1580-1588.

Bevaart, L., Vervoordeldonk, M.J., and Tak, P.P. (2010). Collagen-induced arthritis in mice. Methods Mol. Biol. *602*, 181-192.

Chan, W.C.W., Tan, Z., To, M.K.T., and Chan, D. (2021). Regulation and role of transcription factors in osteogenesis. Int. J. Mol. Sci. *22*, 5445.

Chen, Y.J., Chang, W.A., Hsu, Y.L., Chen, C.H., and Kuo, P.L. (2017). Deduction of novel genes potentially involved in osteoblasts of rheumatoid arthritis using next-generation sequencing and bioinformatic approaches. Int. J. Mol. Sci. *18*, 2396.

Chen, Y.J., Chang, W.A., Wu, L.Y., Hsu, Y.L., Chen, C.H., and Kuo, P.L. (2018). Systematic analysis of transcriptomic profile of chondrocytes in osteoarthritic knee using next-generation sequencing and bioinformatics. J. Clin. Med. *7*, 535.

Cui, J., Dean, D., Wei, R., Hornicek, F.J., Ulmert, D., and Duan, Z. (2020). Expression and clinical implications of leucine-rich repeat containing 15 (LRRC15) in osteosarcoma. J. Orthop. Res. *38*, 2362-2372.

Cunningham, L., Finckbeiner, S., Hyde, R.K., Southall, N., Marugan, J., Yedavalli, V.R., Dehdashti, S.J., Reinhold, W.C., Alemu, L., Zhao, L., et al. (2012). Identification of benzodiazepine Ro5-3335 as an inhibitor of CBF leukemia through quantitative high throughput screen against RUNX1-CBFbeta interaction. Proc. Natl. Acad. Sci. U. S. A. *109*, 14592-14597.

de Bruijn, M.F. and Speck, N.A. (2004). Core-binding factors in hematopoiesis and immune function. Oncogene *23*, 4238-4248.

Galligan, C.L., Baig, E., Bykerk, V., Keystone, E.C., and Fish, E.N. (2007). Distinctive gene expression signatures in rheumatoid arthritis synovial tissue fibroblast cells: correlates with disease activity. Genes Immun. *8*, 480-491.

Ganesan, R. and Rasool, M. (2017). Fibroblast-like synoviocytes-dependent effector molecules as a critical mediator for rheumatoid arthritis: current status and future directions. Int. Rev. Immunol. *36*, 20-30.

Korinfskaya, S., Parameswaran, S., Weirauch, M.T., and Barski, A. (2021). Runx transcription factors in T cells-what is beyond thymic development? Front. Immunol. *12*, 701924.

Malik, N., Yan, H., Moshkovich, N., Palangat, M., Yang, H., Sanchez, V., Cai, Z., Peat, T.J., Jiang, S., Liu, C., et al. (2019). The transcription factor CBFB suppresses breast cancer through orchestrating translation and transcription. Nat. Commun. *10*, 2071.

Manferdini, C., Paolella, F., Gabusi, E., Silvestri, Y., Gambari, L., Cattini, L., Filardo, G., Fleury-Cappellesso, S., and Lisignoli, G. (2016). From osteoarthritic synovium to synovial-derived cells characterization: synovial macrophages are key effector cells. Arthritis Res. Ther. *18*, 83.

Ospelt, C., Gay, S., and Klein, K. (2017). Epigenetics in the pathogenesis of RA. Semin. Immunopathol. *39*, 409-419.

Ray, U., Pathoulas, C.L., Thirusangu, P., Purcell, J.W., Kannan, N., and

Shridhar, V. (2022). Exploiting LRRC15 as a novel therapeutic target in cancer. Cancer Res. *82*, 1675-1681.

Rivellese, F. and Pitzalis, C. (2021). Cellular and molecular diversity in Rheumatoid Arthritis. Semin. Immunol. *58*, 101519.

Sandhu, G. and Thelma, B.K. (2022). New druggable targets for rheumatoid arthritis based on insights from synovial biology. Front. Immunol. *13*, 834247.

Satoh, K., Hata, M., Shimizu, T., Yokota, H., Akatsu, H., Yamamoto, T., Kosaka, K., and Yamada, T. (2005). Lib, transcriptionally induced in senile plaque-associated astrocytes, promotes glial migration through extracellular matrix. Biochem. Biophys. Res. Commun. *335*, 631-636.

Singh, P., Wang, M., Mukherjee, P., Lessard, S.G., Pannellini, T., Carballo, C.B., Rodeo, S.A., Goldring, M.B., and Otero, M. (2021). Transcriptomic and epigenomic analyses uncovered Lrrc15 as a contributing factor to cartilage damage in osteoarthritis. Sci. Rep. *11*, 21107.

Slemmons, K.K., Mukherjee, S., Meltzer, P., Purcell, J.W., and Helman, L.J. (2021). LRRC15 antibody-drug conjugates show promise as osteosarcoma therapeutics in preclinical studies. Pediatr. Blood Cancer *68*, e28771.

Smolen, J.S., Aletaha, D., Barton, A., Burmester, G.R., Emery, P., Firestein, G.S., Kavanaugh, A., McInnes, I.B., Solomon, D.H., Strand, V., et al. (2018). Rheumatoid arthritis. Nat. Rev. Dis. Primers *4*, 18001.

van Hamburg, J.P. and Tas, S.W. (2018). Molecular mechanisms underpinning T helper 17 cell heterogeneity and functions in rheumatoid arthritis. J. Autoimmun. *87*, 69-81.

Wu, Z., Ma, D., Yang, H., Gao, J., Zhang, G., Xu, K., and Zhang, L. (2021). Fibroblast-like synoviocytes in rheumatoid arthritis: surface markers and phenotypes. Int. Immunopharmacol. *93*, 107392.

Xiao, L., Yang, Z., and Lin, S. (2022). Identification of hub genes and transcription factors in patients with rheumatoid arthritis complicated with atherosclerosis. Sci. Rep. *12*, 4677.

Yang, Y., Wu, H., Fan, S., Bi, Y., Hao, M., and Shang, J. (2022). Cancerassociated fibroblastderived LRRC15 promotes the migration and invasion of triplenegative breast cancer cells via Wnt/betacatenin signalling pathway regulation. Mol. Med. Rep. *25*, 2.

You, S., Koh, J.H., Leng, L., Kim, W.U., and Bucala, R. (2018). The tumor-like phenotype of rheumatoid synovium: molecular profiling and prospects for precision medicine. Arthritis Rheumatol. *70*, 637-652.

Zhang, X.P., Ma, J.D., Mo, Y.Q., Jing, J., Zheng, D.H., Chen, L.F., Wu, T., Chen, C.T., Zhang, Q., Zou, Y.Y., et al. (2021). Addition of fibroblast-stromal cell markers to immune synovium pathotypes better predicts radiographic progression at 1 year in active rheumatoid arthritis. Front. Immunol. *12*, 778480.